Pergamon
www.elsevier.com/locate/asr

Adv. Space Res. Vol. 28, No. 5, pp. 729–739, 2001

Printed in Great Britain
0273-1177/01 $20.00 + 0.00

PII: S0273-1177(01)00509-9

ALFVEN WAVE INSTABILITY OF CURRENT SHEETS IN FORCE-FREE PLASMAS: COMPARISON TO ION ACOUSTIC INSTABILITY

P. M. Bellan[1]

[1]*MC 128-95, Caltech, Pasadena CA 91125, USA*

ABSTRACT

Current sheets necessarily form at the interface between adjacent twisted flux tubes and so are ubiquitous to magnetic configurations having non-trivial field topology. In an earlier publication (P. M. Bellan, Phys. Rev. Letters, **83**,4768, 1999) the author showed that current sheets in a low β plasma will be kinetically unstable with respect to Alfvén wave emission if the current sheet becomes sufficiently thin for the field-aligned electron flow to become super-Alfvenic. At first sight it might appear that before the current sheet becomes thin enough to develop a super-Alfvenic flow, ion acoustic instabilities will develop when the sheet becomes thin enough for the electron flow to exceed the ion acoustic velocity. However, it is shown here that because of strong ion Landau damping on ion acoustic waves for plasmas with comparable electron and ion temperatures, ion acoustic waves have a much higher instability threshold than the Alfvén instability. Thus, Alfvén instability should dominate ion acoustic instability in thin current sheets.

Introduction

When two adjacent magnetic flux tubes are twisted, a magnetic rotational discontinuity develops at the interface between the two flux tubes and an associated current sheet is formed (Parker,1983). The rotational discontinuity is parameterized by Δ, the angle of rotation of the magnetic field across the interface (current sheet), and a, the width of the current sheet. The consequences of having such a current sheet in low β plasma were recently considered [Bellan (1999)] using a Vlasov model and it was found that if the current sheet is sufficiently thin, the field-aligned electron flow becomes super-Alfvenic and the system becomes kinetically unstable with respect to Alfvén wave emission (the possibility of current-driven kinetic Alfvén wave instabilities had been examined much earlier for the case of uniform plasmas [Meyerhofer and Perkins, 1984; Cayton, 1985]).

Because the Alfvenic electron flow is confined to the current sheet, the unstable region is confined to the current sheet and so can be viewed as a thin, unstable gain medium embedded in a stable exterior region. The emitted Alfvén waves are inertial Alfvén waves (IAW) if $\beta_e = 2\mu_0 n\kappa T_e/B^2 < m_e/m_i$ and are kinetic Alfvén waves (KAW) if $\beta_e > m_e/m_i$. The emitted waves propagate obliquely out into the exterior region where they are Landau damped. Thus, wave energy created in the current sheet is dissipated in the region exterior to the current sheet. This exterior region damping acts as an effective load on the unstable current sheet and so raises the threshold for instability to be somewhat higher than for a spatially uniform super-Alfvenic electron beam in a spatially uniform background plasma.

The purpose of this paper is to investigate the relationship between Alfvenic and acoustic instabilities in the regime where $\omega << \omega_{ci}$. This is the regime where the magnetohydrodynamic approximation is typically used and so the model presented here provides a kinetic description of situations more commonly described by MHD. Our analysis shows that for plasmas with comparable electron and ion temperatures, the ion acoustic wave has a much higher threshold for instability than the Alfvén wave. Thus, the analysis confirms the picture presented in Bellan (1999) that two colliding twisted flux tubes will spontaneously emit Alfvén waves from their interface when the current sheet at the interface becomes sufficiently thin.

Current Sheet and Alfvenic Electron Flow

Two slowly colliding flux tubes have a current sheet with width a which decreases in time. It seems possible that an ion acoustic kinetic instability might occur before the electrons have attained Alfvenic velocities because acoustic waves are known to become unstable when the electron flow exceeds the ion acoustic velocity $c_s = \sqrt{\kappa T_e/m_i}$. Before proceeding with the wave analysis, we discuss the equilibrium and give the condition for super-Alfvenic field-aligned electron flow (Bellan, 1999).

Because $\beta << 1$, the equilibrium is assumed to be given by $\mathbf{J} \times \mathbf{B} = 0$ or equivalently

$$\nabla \times \mathbf{B} = \alpha(\mathbf{r})\mathbf{B} \tag{1}$$

where

$$\mathbf{B}(\mathbf{x}) = \hat{y}B\sin[\theta(x)] + \hat{z}B\cos[\theta(x)]. \tag{2}$$

Here $\theta(x) = \int_0^x \alpha(x')dx'$ gives the rotation of $\mathbf{B}$ relative to its orientation at $x = 0$. The current sheet corresponds to having α given by

$$\alpha(x) = \frac{\Delta}{a}\Theta(\frac{a}{2} - |x|) \tag{3}$$

where Θ is the Heaviside function. The corresponding field angle dependence is

$$\theta(x) = \begin{cases} \dfrac{x\Delta}{a} & \text{for } |x| \leq a/2 \\ \dfrac{\Delta}{2}\text{sign}(x) & \text{for } |x| \geq a/2 \ . \end{cases} \tag{4}$$

For simplicity, finite Larmor radius effects are neglected by assuming that particles are cold in the direction perpendicular to $\mathbf{B}$. Since the field-aligned current magnitude is $J(x) = \alpha(x)B/\mu_0$, the equilibrium electron flow velocity is

$$u_{\parallel e0}(x) = \frac{\alpha(x)B}{\mu_0 nq} = v_A \frac{c\Delta}{\omega_{pi}a}\ \Theta\left(\frac{a}{2} - |x|\right) \tag{5}$$

where v_A is the Alfvén velocity and terms of order m_e/m_i have been dropped. Thus if $a\omega_{pi}/c < \Delta$, the field-aligned electron flow becomes super-Alfvenic and destabilization of Alfvén waves becomes a possibility.

Mode Identification

We review the dispersion relations of Alfvén waves and ion acoustic waves: In ideal MHD, the Alfvén wave has the dispersion

$$\omega^2 = k_\parallel^2 v_A^2 \tag{6}$$

and there is no parallel electric field. However, when the non-MHD effects of electron inertia and finite parallel electron pressure are taken into account, this dispersion becomes modified to have a dependence on $k_\perp^2$ and there is a finite parallel electric field (Stasiewicz et al., 2000). In the IAW regime the Alfvén wave dispersion becomes $\omega^2 = k_\parallel^2 v_A^2/(1 + k_\perp^2 c^2/\omega_{pe}^2)$ while in the KAW regime the dispersion becomes $\omega^2 = k_\parallel^2 v_A^2(1 + k_\perp^2\rho_s^2)$ where $\rho_s^2 = c_s^2/\omega_{ci}^2$.

Electrostatic waves in the $\omega << \omega_{ci}$ regime have the dispersion (Stix, 1992)

$$k_\perp^2\left(1 + \frac{\omega_{pi}^2}{\omega_{ci}^2}\right) + k_\parallel^2\left(1 - \frac{\omega_{pi}^2}{\omega^2} + \frac{1}{k_\parallel^2\lambda_D^2}\right) = 0. \tag{7}$$

If $k_\perp = 0$, Eq.(7) reverts to the unmagnetized acoustic dispersion $\omega^2 = k_\parallel^2 c_s^2/(1 + k_\parallel^2\lambda_D^2)$ but when $k_\perp \neq 0$ the more complicated dispersion given by Eq.(7) results in ion acoustic waves confined within a conical envelope having cone angle $\sim \omega/\omega_{ci}$ as observed experimentally by Bellan (1976).

Derivation of Wave Equation

We will now reconcile Eqs.(6) and (7) by deriving a wave equation containing both acoustic and Alfvenic physics and then compare the acoustic and Alfvén beam-driven instabilities that would be excited by fast-moving field-aligned electrons in a low β current sheet. Reconciliation of Eqs.(6) and (7) requires retaining displacement current terms normally dropped from low frequency analyses because the displacement current in Ampere's law is equivalent to the left hand side of Poisson's equation, i.e.,

$$\nabla\cdot\left(\mu_0\mathbf{J}+\mu_0\varepsilon_0\frac{\partial\mathbf{E}}{\partial t}-\nabla\times\mathbf{B}\right)=0\Longrightarrow\frac{\partial}{\partial t}\left(\nabla\cdot\mathbf{E}-\frac{1}{\varepsilon_0}\sum_{\sigma=i,e}n_\sigma q_\sigma\right)=0. \tag{8}$$

Thus, retaining displacement current in Ampere's law corresponds to retaining $\nabla\cdot\mathbf{E}$ in Poisson's equation and to retaining the terms $k_\perp^2+k_\parallel^2$ in Eq.(7).

The derivation of the non-uniform plasma Alfvén wave equation given in Bellan (1999) will now be repeated using the full Ampere's law. We assume that perturbed quantities vary as $g(x)\exp(ik_\parallel(x)s-i\omega t)$ where $\omega<<\omega_{ci}$, $k_\parallel=k_z\cos\theta$, and s is the distance along $\mathbf{B}$. The parallel wave current is given by

$$\tilde{J}_\parallel=\sum_\sigma q_\sigma\int dv_\parallel v_\parallel\tilde{f}_\sigma(v_\parallel)=\frac{i\omega\tilde{E}_\parallel}{\mu_0c^2}\sum_\sigma\frac{1}{2k_\parallel^2\lambda_{D\sigma}^2}Z'\left(\frac{\omega-k_\parallel u_{\parallel\sigma0}}{k_\parallel v_{T\sigma}}\right) \tag{9}$$

where Z is the plasma dispersion function and $v_{T\sigma}=\sqrt{2\kappa T_\sigma/m_\sigma}$.

Analysis of perpendicular particle dynamics shows that both electrons and ions have identical $\tilde{\mathbf{E}}\times\mathbf{B}$ drifts which therefore do not result in any perpendicular current. The lowest order perpendicular current thus comes from polarization drift, and since this is proportional to ion mass, the ion polarization drift $\tilde{\mathbf{u}}_{i,pol}=(m_i/q_iB^2)\partial\tilde{\mathbf{E}}/\partial t$ is the dominant contributor to perpendicular current. Thus, the perpendicular wave current is

$$\mu_0\tilde{\mathbf{J}}_\perp=\frac{1}{v_A^2}\frac{\partial\tilde{\mathbf{E}}}{\partial t}. \tag{10}$$

The Alfvén wave polarization is such that the vector potential is $\tilde{\mathbf{A}}=\tilde{A}_\parallel\hat{B}$ and so the perpendicular component of Ampere's law becomes

$$\left[\nabla\left(\nabla\cdot\left(\tilde{A}_\parallel\hat{B}\right)\right)\right]_\perp=\mu_0\tilde{\mathbf{J}}_\perp+\frac{1}{c^2}\frac{\partial\tilde{\mathbf{E}}_\perp}{\partial t} \tag{11}$$

or

$$\nabla_\perp\left(ik_\parallel\tilde{A}_\parallel\right)=\left(\frac{1}{v_A^2}+\frac{1}{c^2}\right)\frac{\partial\tilde{\mathbf{E}}_\perp}{\partial t}. \tag{12}$$

Since the vector potential was assumed to have no perpendicular component, $\tilde{\mathbf{E}}_\perp=-\nabla_\perp\tilde{\phi}$, and so Eq.(12) can be integrated to give

$$k_\parallel\tilde{A}_\parallel=\omega\left(\frac{1}{v_A^2}+\frac{1}{c^2}\right)\tilde{\phi}. \tag{13}$$

Thus, the parallel electric field is

$$\tilde{E}_\parallel=i\omega\left(1-\frac{k_\parallel^2}{\omega^2}\left(\frac{1}{v_A^2}+\frac{1}{c^2}\right)^{-1}\right)\tilde{A}_\parallel \tag{14}$$

and the perpendicular electric field is

$$\tilde{\mathbf{E}}_\perp=-\nabla_\perp\left(\frac{k_\parallel}{\omega}\left(\frac{1}{v_A^2}+\frac{1}{c^2}\right)^{-1}\tilde{A}_\parallel\right). \tag{15}$$

The parallel component of Ampere's law gives

$$-\nabla_\perp^2 \tilde{A}_\parallel = \mu_0 \tilde{J}_\parallel - \frac{i\omega}{c^2}\tilde{E}_\parallel \tag{16}$$

and so substitution of Eq.(9) gives

$$\nabla_\perp^2 \tilde{A}_\parallel = \frac{i\omega \tilde{E}_\parallel}{c^2}\left[1 - \sum_\sigma \frac{1}{2k_\parallel^2 \lambda_{D\sigma}^2} Z'\left(\frac{\omega - k_\parallel u_{\parallel\sigma 0}}{k_\parallel v_{T\sigma}}\right)\right] \tag{17}$$

and then substitution of Eq.(14) gives the wave equation

$$\left(c^2 + v_A^2\right)\nabla_\perp^2 \tilde{A}_\parallel = \left[k_\parallel^2 v_A^2 - \omega^2\left(1 + \frac{v_A^2}{c^2}\right)\right]\left[1 - \sum_\sigma \frac{1}{2k_\parallel^2 \lambda_{D\sigma}^2} Z'\left(\frac{\omega - k_\parallel u_{\parallel\sigma 0}}{k_\parallel v_{T\sigma}}\right)\right]\tilde{A}_\parallel. \tag{18}$$

Comparison of Eq.(18) with Eq.(8) of Bellan (1999) shows that retention of the perpendicular displacement current introduces terms of order v_A^2/c^2 while retention of the parallel displacement current introduces the '1' term in the second square bracket factor.

In both the ion acoustic and KAW regimes the parallel wave phase velocity lies in the range $v_{Ti} << \omega/k_\parallel << v_{T_e}$ so that after using the appropriate asymptotic forms of Z', the wave equation becomes

$$\begin{aligned}\left(c^2 + v_A^2\right)\nabla_\perp^2 \tilde{A}_\parallel &= \left[k_\parallel^2 v_A^2 - \omega^2\left(1 + \frac{v_A^2}{c^2}\right)\right] \times \\ &\left\{1 + \frac{1}{k_\parallel^2 \lambda_{De}^2}\left[1 - \frac{k_\parallel^2 c_s^2}{\omega^2} + i\pi^{1/2}\left(\bar{\xi}_e \exp(-\bar{\xi}_e^2) + \frac{T_e}{T_i}\xi_i \exp(-\xi_i^2)\right)\right]\right\}\tilde{A}_\parallel \end{aligned} \tag{19}$$

where

$$\bar{\xi}_e = \frac{\omega - k_\parallel u_{\parallel e0}}{k_\parallel v_{Te}}, \quad \xi_i = \frac{\omega}{k_\parallel v_{Ti}}. \tag{20}$$

Correspondence of Wave Equation to Familiar Limits

The general nature of Eq.(19) will now be established by showing that it corresponds to several familiar limiting cases:

1. If the plasma is uniform and $\nabla_\perp = 0$ (no wave dependence on coordinates transverse to the magnetic field), then the acoustic and Alfvén waves decouple and Eq.(19) gives the two dispersion relations $\omega^2 = k_\parallel^2 v_A^2 / \left(1 + v_A^2/c^2\right)$ and $\omega^2 = k_\parallel^2 c_s^2 / \left(1 + k_\parallel^2 \lambda_{De}^2\right)$. If the imaginary terms (Landau terms) are included, then the usual ion acoustic instability is recovered, i.e., if $u_{\parallel e0} > c_s$ and $T_e >> T_i$ then ion acoustic waves are destabilized.

2. In the limit of zero plasma density, $1/\lambda_{D\sigma}^2 \to 0$ and $v_A^2/c^2 \to \infty$ so that Eq.(19) reverts to $\nabla_\perp^2 \tilde{A}_\parallel = \left(k_\parallel^2 - \omega^2/c^2\right)\tilde{A}_\parallel$, i.e., to an electromagnetic wave in vacuum.

3. If the plasma is uniform and an $\exp(i\mathbf{k}_\perp \cdot \mathbf{x})$ dependence is assumed, then using $\rho_s^2 = c^2\lambda_{De}^2/v_A^2$, Eq.(19) becomes the dispersion relation

$$k_\perp^2 \rho_s^2 = \left[\frac{\omega^2}{k_\parallel^2 v_A^2} - \frac{1}{\left(1 + v_A^2/c^2\right)}\right]\left[1 + k_\parallel^2 \lambda_{De}^2 - \frac{k_\parallel^2 c_s^2}{\omega^2} + i\pi^{1/2}\left(\bar{\xi}_e \exp(-\bar{\xi}_e^2) + \frac{T_e}{T_i}\xi_i \exp(-\xi_i^2)\right)\right]. \tag{21}$$

This can be solved graphically by plotting $k_\perp^2 \rho_s^2$ versus $k_\parallel^2 v_A^2/\omega^2$ and using $c_s^2 = \beta_e v_A^2/2$; the case for $\beta_e = 0.1$ is plotted in Figure 1.

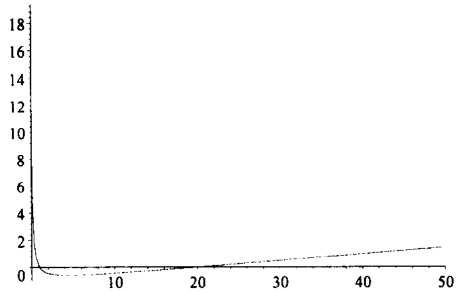

Figure 1. Plot of $k_\perp^2\rho_s^2$ versus $k_\parallel^2 v_A^2/\omega^2$ for $\beta_e = 0.1$; the downward sloping curve on the left is the kinetic Alfvén wave while the upward sloping curve on the right is the acoustic wave.

For clarity, the imaginary terms have been omitted in Figure 1. This figure shows that for a given $\mathbf{k} = k_\parallel\hat{B} + \mathbf{k}_\perp$, the acoustic and Alfvén waves are well separated in frequency and so Eq.(21) can be solved approximately by assuming either $\omega^2 \sim k_\parallel^2 c_s^2$ or else $\omega^2 \sim k_\parallel^2 v_A^2$ (note that the frequency of the Alfvén wave exceeds by a factor $\beta_e^{-1/2}$ the frequency of an acoustic wave having the same $\mathbf{k} = k_\parallel\hat{B} + \mathbf{k}_\perp$). Hence, if we assume $\omega^2 \sim k_\parallel^2 c_s^2$, Eq.(21) becomes

$$k_\perp^2\rho_s^2 + k_\perp^2\lambda_{De}^2 + 1 + k_\parallel^2\lambda_{De}^2 - \frac{k_\parallel^2 c_s^2}{\omega^2} + i\pi^{1/2}\left(\bar{\xi}_e\exp(-\bar{\xi}_e^2) + \frac{T_e}{T_i}\xi_i\exp(-\xi_i^2)\right) = 0; \tag{22}$$

which is just Eq.(7) with Landau damping/instability added. It should be noted that the $k_\perp^2\lambda_{De}^2$ term resulted from retaining v_A^2/c^2 in Eq.(21).

On the other hand if we assume that $\omega^2 \sim k_\parallel^2 v_A^2$, then Eq.(21) becomes

$$k_\perp^2\rho_s^2 - \left[\frac{\omega^2}{k_\parallel^2 v_A^2} - \frac{1}{(1+v_A^2/c^2)}\right]\left[1 + k_\parallel^2\lambda_{De}^2 + i\pi^{1/2}\left(\bar{\xi}_e\exp(-\bar{\xi}_e^2) + \frac{T_e}{T_i}\xi_i\exp(-\xi_i^2)\right)\right] = 0 \tag{23}$$

which is just the KAW dispersion

$$\omega^2 = k_\parallel^2 v_A^2(1 + k_\perp^2\rho_s^2) \tag{24}$$

generalized to include Landau damping/instability and terms of order v_A^2/c^2 and $k_\parallel^2\lambda_{De}^2$.

Comparison of growth rates of KAW and ion acoustic instabilities

The dispersion relations above can be cast in the form $\varepsilon_r(\omega_r + i\omega_i) + i\varepsilon_i(\omega_r + i\omega_i) = 0$ so that $\omega_i = -\varepsilon_i/\left(\partial\varepsilon_r(\omega_r)/\partial\omega_r\right)$. From Eq.(22) the real part of the acoustic frequency is

$$\omega_r = \frac{k_\parallel c_s}{\sqrt{1 + k_\perp^2\rho_s^2 + k^2\lambda_{De}^2}} \tag{25}$$

and so the acoustic growth rate is

$$\omega_i = -\frac{k_\parallel c_s \pi^{1/2}\left(\bar{\xi}_e\exp(-\bar{\xi}_e^2) + \frac{T_e}{T_i}\xi_i\exp(-\xi_i^2)\right)}{2\left(1 + k_\perp^2\rho_s^2 + k^2\lambda_{De}^2\right)^{3/2}} \tag{26}$$

or, using Eq.(20),

$$\omega_i = -\left(\frac{\pi}{8}\right)^{1/2}\left(\frac{m_e}{m_i}\right)^{1/2} k_{\|} c_s \times \left\{ \frac{\left(1-\frac{u_{\|e0}}{c_s}\sqrt{1+k_\perp^2\rho_s^2+k^2\lambda_{De}^2}+\left(\frac{T_e}{T_i}\right)^{3/2}\left(\frac{m_i}{m_e}\right)^{1/2}\exp\left[-\frac{T_e/2T_i}{\left(1+k_\perp^2\rho_s^2+k^2\lambda_{De}^2\right)}\right]\right)}{\left(1+k_\perp^2\rho_s^2+k^2\lambda_{De}^2\right)^2} \right\} \tag{27}$$

which is just the finite $k_\perp^2\rho_s^2$ generalization of Eq. (9.7.3) of Krall and Trivelpiece (1972).

Similarly, the KAW growth rate may be written as

$$\omega_i = -k_{\|}^2 v_A^2 k_\perp^2 \rho_s^2 \frac{\pi^{1/2}\left(\bar{\xi}_e \exp(-\bar{\xi}_e^2)+\frac{T_e}{T_i}\xi_i \exp(-\xi_i^2)\right)}{2\omega} \tag{28}$$

or, using Eqs.(20), (24), and $\omega_r^2 = k_{\|}^2 v_A^2(1+k_\perp^2\rho_s^2)$,

$$\omega_i = -\left(\frac{\pi}{\beta_e}\right)^{1/2}\left(\frac{m_e}{m_i}\right)^{1/2} k_\perp^2\rho_s^2 \frac{\left(1-\frac{u_{\|e0}}{v_A\sqrt{1+k_\perp^2\rho_s^2}}+\left(\frac{T_e}{T_i}\right)^{3/2}\left(\frac{m_i}{m_e}\right)^{1/2}\exp\left[-\frac{(1+k_\perp^2\rho_s^2)}{\beta_e}\frac{T_e}{T_i}\right]\right)}{2} k_{\|} v_A. \tag{29}$$

Comparison of Eqs.(27) and (29) shows that while the Alfvén and ion acoustic growth rates are formally similar, the Alfvén growth rate has a lower threshold because the Alfvén wave has negligible ion Landau damping due to the β_e^{-1} factor in the argument of the exponential in Eq.(29).

A quantitative comparison can be made by considering a hydrogen plasma with $T_e/T_i = 1$. Since the current sheet acts as a lossy gain region that is coupled to the exterior region (much like a laser cavity coupled via partially reflecting mirrors to the outside world), the lowest order $k_\perp$ mode in the current sheet will be approximately a half-wavelength, i.e., $k_\perp a \sim \pi$; for example, see Fig. 1 of Bellan (1999). At marginal instability of Alfvén waves, $a \approx \Delta c/\omega_{pi}$ and so the perpendicular wavelength will be $k_\perp \sim \pi/a \sim \pi\omega_{pi}/\Delta c$ giving

$$k_\perp^2\rho_s^2 \sim \left(\frac{\pi}{\Delta}\right)^2 \frac{\beta_e}{2}. \tag{30}$$

Thus, the example used in Bellan (1999) where $\beta_e = 0.1$ and $\Delta = 0.87\pi$ corresponds to having $k_\perp^2\rho_s^2 \sim 0.1$ in the current sheet. Figure 2 plots $\omega_i/k_{\|}v_A$ versus $u_{\|e0}/v_A$ for acoustic and KAW waves for these parameters and shows that the Alfvén wave has a much lower instability threshold than the ion acoustic wave.

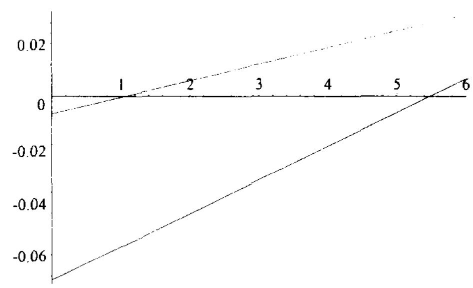

Figure 2. Comparison of acoustic and kinetic Alfven wave growth rates $\omega_i/k_{\|}v_A$ versus $u_{\|e0}/v_A$ for a hydrogen plasma with $\beta_e = 0.1$, $T_e/T_i = 1$, $k_\perp^2\rho_s^2 = 0.1$, $k^2\lambda_{De}^2 << 1$. Upper curve is the Alfvén growth rate while lower curve is the ion acoustic growth rate. The Alfvén wave has a lower threshold for instability.

IAW regime

In the IAW regime $\beta < m_e/m_i$ and the Alfvén wave parallel phase velocity is faster than the electron thermal velocity, i.e., $\omega/k_\parallel >> v_{Te}$. However, the acoustic wave parallel phase velocity will be slower than the electron thermal velocity (because of lower frequency). Thus, the acoustic dispersion relation is still given by Eq.(22) and still has growth rate given by Eq.(27). The situation for the IAW dispersion is more complicated. Inside the current sheet $\bar{\xi}_e$ is less than unity because $u_{\parallel e0} \approx \omega/k_\parallel$ whereas outside the current sheet ξ_e is much larger than unity because $\omega/k_\parallel >> v_{Te}$. Thus, because of the fast electron beam inside the current sheet the IAW actually behaves like the KAW, whereas outside the current sheet the IAW behaves in the normal fashion. Thus, the instability threshold for the IAW will again be lower than for the acoustic wave, but the IAW growth will be smaller than a KAW having the same Δ because the $k_\perp^2\rho_s^2$ factor in Eq.(29) is smaller for an IAW.

Summary

Current sheets arise when two distinct field topologies collide or when magnetic flux tubes become braided. The current sheet forms because of the rotational discontinuity of the magnetic field at the interface between two adjacent, distinct magnetic structures. Current sheets in low β plasmas will have mainly field-aligned currents and hence field-aligned electron flow. As a current sheet becomes narrower, the field-aligned electron flow is squeezed into a smaller channel so that the velocity of the flow increases. If the electron flow velocity becomes super-Alfvenic, Alfvén waves become destabilized via inverse Landau damping.

One might expect that ion acoustic waves would also be destabilized by this fast electron flow and would have a lower threshold for instability than Alfvén waves because the sound velocity c_s is much smaller than the Alfvén velocity v_A. However, this does not happen because ion Landau damping is much stronger for acoustic waves than for Alfvén waves and so inhibits acoustic instability but not Alfvén instability. Thus, the acoustic instability threshold is much higher than the Alfvén threshold for situations with comparable ion and electron temperatures. Thin current sheets will consequently emit Alfvén waves, but not ion acoustic waves; the emitted Alfvén waves will transport magnetic twist away from the current sheet and so alter the magnetic topology.

ACKNOWLEDGMENTS

Supported by USDOE.

APPENDIX

This appendix is in response to a referee's question regarding how the ion acoustic mode discussed in this paper relates to the "slow ion acoustic" (SIA) mode discussed by Seyler and Wahlund (1996) and Seyler, Clark, Bonnell and Wahlund (1998).

To show this relationship we derive the 2-fluid dispersion relation from the linearized continuity equation and warm-plasma equation of motion,

$$-i\omega\tilde{n}_\sigma + i\mathbf{k}\cdot\tilde{\mathbf{u}}_\sigma n_\sigma = 0 \tag{31}$$

$$-i\omega m_\sigma\tilde{\mathbf{u}}_\sigma = q_\sigma\left(-i\mathbf{k}\tilde{\phi}+\tilde{\mathbf{u}}_\sigma\times\mathbf{B}\right) - i\mathbf{k}\gamma\frac{\tilde{n}}{n}\kappa T_\sigma, \tag{32}$$

where σ denotes species, $\gamma = 1$ for isothermal phenomena, and $\gamma = 3$ for adiabatic phenomena. Solution of Eq. (32) gives the velocity

$$\tilde{\mathbf{u}}_\sigma = \left(k_z\hat{z} + \frac{\mathbf{k}_\perp}{1-\omega_{c\sigma}^2/\omega^2} + \frac{q_\sigma\mathbf{B}}{i\omega m_\sigma}\times\frac{\mathbf{k}}{1-\omega_{c\sigma}^2/\omega^2}\right)\frac{\left(q_\sigma\tilde{\phi} + \frac{\tilde{n}_\sigma}{n}\gamma\kappa T_\sigma\right)}{\omega m_\sigma} \tag{33}$$

which can be combined with Eq.(31) to obtain

$$\frac{\tilde{n}_\sigma}{n} = \left(\frac{k_z^2 + \dfrac{k_\perp^2}{1-\omega_{c\sigma}^2/\omega^2}}{1 - \left(k_z^2 + \dfrac{k_\perp^2}{1-\omega_{c\sigma}^2/\omega^2}\right)\dfrac{\gamma_\sigma \kappa T_\sigma}{\omega^2 m_\sigma}} \right) \frac{q_\sigma \tilde{\phi}}{\omega^2 m_\sigma}. \tag{34}$$

Substituting Eq.(34) into Poisson's equation gives the 2-fluid, warm magnetized plasma dispersion relation

$$k^2 = \left(\frac{\dfrac{k_z^2}{\omega^2} + \dfrac{k_\perp^2}{\omega^2 - \omega_{ci}^2}}{1 - \left(\dfrac{k_z^2}{\omega^2} + \dfrac{k_\perp^2}{\omega^2-\omega_{ci}^2}\right)\dfrac{\gamma_i \kappa T_i}{m_i}} \right)\omega_{pi}^2 + \left(\frac{\dfrac{k_z^2}{\omega^2} + \dfrac{k_\perp^2}{\omega^2 - \omega_{ce}^2}}{1 - \left(\dfrac{k_z^2}{\omega^2} + \dfrac{k_\perp^2}{\omega^2-\omega_{ce}^2}\right)\dfrac{\gamma_e \kappa T_e}{m_e}} \right)\omega_{pe}^2. \tag{35}$$

The wave frequency is assumed small compared to the ion cyclotron frequency, i.e. $\omega << \omega_{ci}$, for the present discussion.

Conventional Ion Acoustic Mode

Ions: We assume cold ions so that $\omega/k_z >> \sqrt{\kappa T_i/m_i}$ and $k_\perp r_{Li} << 1$ (where $r_{Li} = \sqrt{\kappa T_i/m_i}/\omega_{ci}$ is the ion Larmor radius); thus thermal terms in the ion term of Eq.(35) can be dropped.

Electrons: The electrons are warm so that $\omega/k_z << \sqrt{\kappa T_e/m_e}$ and the '1' can be dropped from the electron term which becomes Boltzmann-like (also $\gamma_e = 1$).

Using these assumptions, Eq.(35) reduces to

$$k_\perp^2 + k_z^2 = \left(\frac{k_z^2}{\omega^2} + \frac{k_\perp^2}{\omega^2 - \omega_{ci}^2}\right)\omega_{pi}^2 - \frac{1}{\lambda_{De}^2} \tag{36}$$

which becomes Eq.(7) in the $\omega << \omega_{ci}$ limit.

Slow Ion Acoustic Mode

Ions: It is assumed that k_z^2 can be dropped from the ion term in Eq.(35), i.e., $k_z^2/\omega^2 << k_\perp^2/\left|\omega^2 - \omega_{ci}^2\right|$.

Electrons: It is assumed that $k_z^2/\omega^2 >> k_\perp^2/\left|\omega^2 - \omega_{ce}^2\right|$.

Using these two assumptions, Eq.(35) reduces to

$$k^2 = \frac{k_\perp^2}{\left(\omega^2 - \omega_{ci}^2 - k_\perp^2 \dfrac{\gamma_i \kappa T_i}{m_i}\right)}\omega_{pi}^2 + \frac{k_z^2}{\left(\omega^2 - k_z^2 \dfrac{\gamma_e \kappa T_e}{m_e}\right)}\omega_{pe}^2 \tag{37}$$

which, except for the added γ's, is identical to Eq. (7) of Seyler and Wahlund (1996).

Assuming quasineutrality amounts to dropping the k^2 on the LHS. Balancing the RHS terms gives the dispersion

$$\omega^2 = \frac{\omega_{ci}^2 + k_\perp^2\left(\dfrac{\gamma_i \kappa T_i + \gamma_e \kappa T_e}{m_i}\right)}{1 + \dfrac{m_e}{m_i}\dfrac{k_\perp^2}{k_z^2}}. \tag{38}$$

Seyler et al. define the SIA as the mode corresponding to the limit $m_e k_\perp^2/m_i k_z^2 >> 1$, so that Eq.(38) becomes

$$\frac{\omega}{\omega_{ci}} = \frac{k_z m_i^{1/2}}{k_\perp^2 m_e^{1/2}}\sqrt{1 + k_\perp^2 \rho_s^2} \tag{39}$$

where $\rho_s^2 = (\gamma_i \kappa T_i + \gamma_e \kappa T_e)/m_i \omega_{ci}^2$. Seyler et al.(1998) plot the SIA mode for $k_z m_i^{1/2}/k_\perp m_e^{1/2} = 0.1$ in their Fig. 1. We note that Eq.(39) can also be written as

$$\omega^2 = \frac{k_z^2 v_A^2}{k_\perp^2 c^2/\omega_{pe}^2}\left(1 + k_\perp^2 \rho_s^2\right) \tag{40}$$

and so simply corresponds to the finite $k_\perp \rho_s$ extension of the electrostatic limit of the inertial Alfvén wave [dispersion $\omega^2 = k_z^2 v_A^2/(1 + k_\perp^2 c^2/\omega_{pe}^2)$].

Kinetic Analysis of SIA mode

It is important to check that this 2-fluid SIA mode is consistent with the more accurate model provided by the magnetized plasma kinetic electrostatic dispersion relation,

$$1 + \sum_\sigma \frac{e^{-k_\perp^2 r_{L\sigma}^2}}{k^2 \lambda_{D\sigma}^2} \sum_{n=-\infty}^{\infty} I_n\left(k_\perp^2 r_{L\sigma}^2\right)\left[1 + \alpha_{0\sigma} Z(\alpha_{n\sigma})\right] = 0 \tag{41}$$

where $\alpha_n = (\omega - n\omega_{c\sigma})/v_{T\sigma}$ and $v_{T\sigma} = \sqrt{2\kappa T_\sigma/m_\sigma}$. Equation (39) implies

$$\frac{\omega^2}{k_z^2} > \frac{\gamma_i \kappa T_i + \gamma_e \kappa T_e}{m_e} > v_{Te} >> v_{T_i} \tag{42}$$

showing that the large argument limit should be used for evaluating both $Z(\alpha_{ne})$ and $Z(\alpha_{ni})$ in Eq.(41). Thus the 2-fluid SIA dispersion corresponds to assuming $\omega/k_z v_{Te} >> 1$, $\omega/k_z v_{Ti} >> 1$, $k_\perp^2 r_{Le}^2 << 1$, and $\omega/\omega_{ci} << 1$. Because $v_{Te} >> v_{T_i}$, finite $k_z v_{Te}/\omega$ terms should be kept as a higher order correction for the electrons, but $k_z v_{Ti}/\omega$ terms are entirely negligible for ions and may be dropped.

Since ion and electron responses differ, it is useful to define a generic susceptibility

$$\begin{aligned}
\chi_\sigma &= \frac{e^{-k_\perp^2 r_{L\sigma}^2}}{k^2 \lambda_{D\sigma}^2} \sum_{n=-\infty}^{\infty} I_n\left(k_\perp^2 r_{L\sigma}^2\right)\left[1 + \alpha_{0\sigma} Z(\alpha_{n\sigma})\right] \\
&= \frac{e^{-k_\perp^2 r_{L\sigma}^2}}{k^2 \lambda_{D\sigma}^2}\left(I_0\left(k_\perp^2 r_{L\sigma}^2\right)\left[1 + \alpha_{0\sigma} Z(\alpha_{o\sigma})\right] + \sum_{n=1}^{\infty} I_n\left(k_\perp^2 r_{L\sigma}^2\right)\left[2 + \alpha_{0\sigma}\left(Z(\alpha_{n\sigma}) + Z(\alpha_{-n\sigma})\right)\right]\right).
\end{aligned} \tag{43}$$

Using the large argument expansion for the plasma dispersion function

$$Z(\alpha) = -\frac{1}{\alpha}\left[1 + \frac{1}{2\alpha^2} + \frac{3}{4\alpha^4} + ...\right] + i\pi^{1/2}\exp(-\alpha^2) \tag{44}$$

and ignoring Landau damping terms, it is seen that

$$1 + \alpha Z(\alpha) = -\frac{1}{2\alpha^2}\left[1 + \frac{3}{2\alpha^2} + ...\right] \tag{45}$$

and

$$2 + \alpha_{0\sigma}\left(Z(\alpha_{n\sigma}) + Z(\alpha_{-n\sigma})\right) = -\frac{2n^2\omega_{c\sigma}^2}{\omega^2 - n^2\omega_{c\sigma}^2}. \tag{46}$$

The $k_z v_{Ti}/\omega << 1$ assumption allows dropping the $n = 0$ term from the ion susceptibility which reduces to the Bernstein wave form

$$\chi_i = -2\frac{e^{-k_\perp^2 r_{Li}^2}}{k^2 \lambda_{Di}^2}\left(\sum_{n=1}^{\infty} I_n\left(k_\perp^2 r_{Li}^2\right)\frac{n^2\omega_{ci}^2}{\omega^2 - n^2\omega_{ci}^2}\right). \tag{47}$$

Invoking the $k_\perp^2 r_{Le}^2 << 1$ assumption, retaining finite $k_z v_{Te}/\omega$, and using $v_{Te}^2/2\lambda_{De}^2 = r_{Le}^2\omega_{ce}^2/\lambda_{De}^2 = \omega_{pe}^2$ the electron susceptibility becomes

$$\begin{aligned}
\chi_e &= \frac{1}{k^2 \lambda_{De}^2}\left(-\frac{k_z^2 v_{Te}^2}{2\omega^2}\left(1 + \frac{3k_z^2 v_{Te}^2}{2\omega^2}\right) - k_\perp^2 r_{L\sigma}^2 \frac{\omega_{ce}^2}{\omega^2 - \omega_{ce}^2}\right) \\
&= -\frac{k_z^2 \omega_{pe}^2}{k^2\omega^2}\left(1 + 3k_z^2\lambda_{De}^2\frac{\omega_{pe}^2}{\omega^2}\right) - \frac{k_\perp^2}{k^2}\frac{\omega_{pe}^2}{\omega^2 - \omega_{ce}^2}
\end{aligned} \tag{48}$$

so Eq.(41) becomes

$$1-2\frac{e^{-k_\perp^2 r_{Li}^2}}{k^2\lambda_{Di}^2}\left(\sum_{n=1}^{\infty} I_n\left(k_\perp^2 r_{Li}^2\right)\frac{n^2\omega_{ci}^2}{\omega^2-n^2\omega_{ci}^2}\right)-\frac{k_z^2}{k^2}\frac{\omega_{pe}^2}{\omega^2}\left(1+3k_z^2\lambda_{De}^2\frac{\omega_{pe}^2}{\omega^2}\right)-\frac{k_\perp^2}{k^2}\frac{\omega_{pe}^2}{\omega^2-\omega_{ce}^2}=0. \tag{49}$$

If one considers the $\omega << \omega_{ci}$, $k_\perp^2 r_{Li}^2 << 1$ expansion of the $n=1$ term of the ion susceptibility one obtains

$$\begin{aligned}
-2\frac{e^{-k_\perp^2 r_{Li}^2}}{k^2\lambda_{Di}^2} I_1\left(k_\perp^2 r_{Li}^2\right)\frac{\omega_{ci}^2}{\omega^2-\omega_{ci}^2} &\simeq \frac{k_\perp^2}{k^2}\left(1-k_\perp^2 r_{Li}^2\right)\frac{\omega_{pi}^2}{\omega_{ci}^2}\\
&\simeq \frac{k_\perp^2}{k^2}\frac{\omega_{pi}^2}{\left(\omega_{ci}^2+k_\perp^2\dfrac{\kappa T_i}{m_i}\right)}\\
&= \frac{1}{k^2\lambda_{Di}^2}\frac{k_\perp^2 r_{Li}^2}{\left(1+k_\perp^2 r_{Li}^2\right)}
\end{aligned} \tag{50}$$

where the middle line corresponds to the $\omega << \omega_{ci}$ limit of the ion term in Eq.37. Thus, the 2-fluid SIA mode corresponds to the $k_\perp^2 r_{Li}^2 << 1$, $\omega/\omega_{ci} << 1$ limit of the $n=1$ ion term. Curiously, the last two lines of Eq.(50) and hence the 2-fluid expression, Eq.(39) turn out to be valid even in the limit $k_\perp^2 r_{Li}^2 >> 1$. This limit corresponds to a Boltzmann-like ion response as noted by Seyler and Wahlund (1996).

To prove that the last two lines of Eq.(50) are in fact valid for all values of $k_\perp^2 r_{Li}^2$, consider the identity

$$1=\sum_{n=-\infty}^{\infty} I_n(x)\,e^{-x}=I_0(x)e^{-x}+2\sum_{n=1}^{\infty} I_n(x)\,e^{-x} \tag{51}$$

so that in the $\omega << \omega_{ci}$ limit, χ_i becomes

$$\begin{aligned}
\lim_{\omega/\omega_{ci}\to 0}\chi_i &= 2\frac{e^{-k_\perp^2 r_{Li}^2}}{k^2\lambda_{Di}^2}\sum_{n=1}^{\infty} I_n\left(k_\perp^2 r_{Li}^2\right)\\
&= \frac{1}{k^2\lambda_{Di}^2}\left[1-I_0(k_\perp^2 r_{Li}^2)e^{-k_\perp^2 r_{Li}^2}\right].
\end{aligned} \tag{52}$$

We note that the form $1-I_0(k_\perp^2 r_{Li}^2)e^{-k_\perp^2 r_{Li}^2}$ conventionally occurs as the finite Larmor radius correction to low frequency perpendicular motion and, for example, has been discussed by Lysak and Lotko (1996) in conjunction with Alfvén waves.

Now, one might naively expect that the fluid approximation as given in the last line of Eq.(50) would be invalid for large $k_\perp^2 r_{Li}^2$ because (i) Eq.(50) comes from just the $n=1$ term in the infinite sum, (ii) Eq.(50) was derived on the assumption that $k_\perp^2 r_{Li}^2 << 1$, and (iii) the last line of Eq.(50) looks quite different from the last line of Eq.(52), the kinetic expression which includes all cyclotron harmonics. However, direct numerical evaluation shows that the two functions $x/(1+x)$ and $1-I_0(x)e^{-x}$ are the same within 7% over the entire range $0 < x < \infty$. It is interesting that approximating $1-I_0(x)e^{-x} \simeq x/(1+x)$ is, in general, far more accurate than the commonly used Taylor expansion $1-I_0(x)e^{-x} \approx x-3x^2/4$ which is valid only for $x << 1$ and even in that range is only a trifle better representation than the $x/(1+x)$ representation. Thus, the last line of Eq.(50) is an excellent approximation to the kinetic limit for all $k_\perp^2 r_{Li}^2$.

The kinetic dispersion can therefore be written as

$$k^2=-\frac{1}{\lambda_{Di}^2}\left(1-I_0(k_\perp^2 r_{Li}^2)e^{-k_\perp^2 r_{Li}^2}\right)+\frac{k_z^2\omega_{pe}^2}{\omega^2}\left(1+3k_z^2\lambda_{De}^2\frac{\omega_{pe}^2}{\omega^2}\right)-k_\perp^2\frac{\omega_{pe}^2}{\omega_{ce}^2}. \tag{53}$$

Using $1-I_0(x)e^{-x} \simeq x/(1+x)$ this can be expressed as

$$\omega^2=\omega_{pe}^2\frac{\left(1+3k_z^2\lambda_{De}^2\dfrac{\omega_{pe}^2}{\omega^2}\right)}{1+\dfrac{k_\perp^2}{k_z^2}\left(1+\dfrac{1}{1+k_\perp^2 r_{Li}^2}\dfrac{\omega_{pi}^2}{\omega_{ci}^2}+\dfrac{\omega_{pe}^2}{\omega_{ce}^2}\right)}. \tag{54}$$

Assuming $k_\perp^2/k_z^2 >> 1$, $k_\perp^2 r_{Li}^2 << \omega_{pi}^2/\omega_{ci}^2$, and $k_\perp^2 r_{Li}^2 << m_i/m_e$ this reduces to

$$\omega^2 = \frac{k_z^2 v_A^2}{k_x^2 c^2/\omega_{pe}^2}\left(1 + 3k_z^2\lambda_{De}^2\frac{\omega_{pe}^2}{\omega^2}\right)\left(1 + k_\perp^2 r_{Li}^2\right). \tag{55}$$

By assumption, the term $3k_z^2\lambda_{De}^2\omega_{pe}^2/\omega^2$ is small, and so we solve Eq.(55) iteratively. When the first approximation $\omega^2 = \omega_{pe}^2 k_z^2 v_A^2\ (1 + k_\perp^2 r_{Li}^2)/k_x^2 c^2$ is substituted into Eq.(55), we obtain

$$\omega^2 = \frac{k_z^2 v_A^2}{k_x^2 c^2/\omega_{pe}^2}\left(1 + k_\perp^2 \rho_s^2\right) \tag{56}$$

where

$$\rho_s^2 = r_{Li}^2\left(1 + 3\frac{T_e}{T_i}\right). \tag{57}$$

This shows that the correct choices of the γ's for the fluid equations are $\gamma_i = 1$ and $\gamma_e = 3$. The dispersion is consistent with $\omega << \omega_{ci}$ provided $(1 + k_\perp^2\rho_s^2)\, k_z^2 m_i/k_\perp^2 m_e << 1$. Thus, Eq.(56) agrees with the 2-fluid mode, and again is simply a warm plasma extension of the electrostatic limit of the inertial Alfvén wave. Equation (56) is valid for $k_\perp^2 r_{Li}^2 << \omega_{pi}^2/\omega_{ci}^2$ which corresponds to $k_\perp^2\lambda_{Di}^2 << 1$.

REFERENCES

Bellan, P. M., Resonance Cones below the Ion Cyclotron Frequency: Theory and Experiment, *Phys. Rev. Letters,* **37,** 903-906, 1976.

Bellan, P. M., Alfvén Wave Instability of Current Sheets in Force-Free Collisionless Plasmas, *Phys. Rev. Letters,* **83,** 4768-4771, 1999.

Cayton, T. E., Current-driven instabilities in the fluid limit: Parallel kinetic effects in reversed field pinches, *Phys. Fluids* **28**, 598-610, 1985.

Krall, N. A. and Trivelpiece, A. W., Principles of Plasma Physics, McGraw Hill Book Company, New York, NY, 1972.

Lysak, R. L. and Lotko, W., On the kinetic dispersion relations for shear Alfvén waves, *J. Geophys. Res.* **101**, 5085-5094, 1996.

Meyerhofer, D. D. and Perkins, F. W., Current-driven instabilities of the kinetic shear Alfvén wave – application to reversed field pinches and spheromaks, *Phys. Fluids* **27**, 2483-2492, 1984.

Parker, E. N., Magnetic Current Sheets in Evolving Fields I. General Theory, *Astrophys. J.*, **264**, 635-641, 1983.

Seyler, C. E. and Wahlund, J.-E., Theory of nearly perpendicular electrostatic plasma waves and comparison to Freja satellite observations, *J. Geophys. Res.*, **101**, 21795-21813, (1996).

Seyler, C. E., Clark, A. E., Bonnell, J. and Wahlund, J.-E., Electrostatic broadband ELF wave emission by Alfvén wave breaking, *J. Geophys. Res.*, **103**, 7027-7041, 1998.

Stasiewicz, K., Bellan, P., Chaston, C., Kletzing, C., Lysak, R., Maggs, J., Pokhotelov, O., Seyler, C., Shukla, P., Stenflo, L., Streltsov, A., and Wahlund, J.-E., Small scale Alfvenic structure in the aurora, *Space Science Rev.*, **92**, 423-533, 2000.

Stix, T. H., Waves in Plasmas, American Institute of Physics Press, New York, NY, 1992; p.62, Eq. (58).